



Rapid Segmentation of the Median Nerve for a Video-Guided Ultrasound System

Aaron Sun¹, Vikas Shivaprabhu¹, Jihang Wang¹, John Galeotti^{1,3}, Vijay Gorantla², George Stetten^{1,3}
Departments of Bioengineering¹ and Reconstructive Surgery², University of Pittsburgh
Robotics Institute, Carnegie Mellon University³



INTRODUCTION

The recent development of high resolution ultrasound (HRUS) has allowed for the imaging of individual nerve fascicles, which introduces a realm of new possibilities for the monitoring of nerve regeneration and regrowth following peripheral nerve injury (PNI) or vascularized composite allotransplantation (VCA). A rapid, non-invasive, and inexpensive procedure afforded by HRUS to objectively diagnose repair and regrowth of nerves would be a significant step forward in studying and providing treatment to these patients. In order to achieve this, a way to reliably identify and quantify fascicular structures must first be developed.

We seek to provide a rapid yet effective method towards segmentation that lends itself to parallelization through GPU technology. In this particular application, the target is identification of fascicles in 2D and 3D high resolution ultrasounds (HRUS) of the median nerve at 50 MHz as part of a new system combining video from a probe-mounted camera with ultrasound data to monitor the progression of blood vessels and nerves after reconstructive surgery. We believe that our method will be effective despite the challenges of segmenting ultrasound data: high noise, incomplete boundaries, and computationally expensive data sets.

The method involves three parts: formation of pixel clusters (patches), identification of boundary points and medial points, and segmentation by grouping.

FORMATION OF PIXEL CLUSTERS

We begin by constructing patches of homogeneous pixels using a directed graph of edges between neighboring pixels in order to reduce noise and subsequent computational cost while preserving meaningful structures. Pixel intensity as well as variance are factored into a descending variance graph, where the variance and mean are calculated within a sphere of radius r centered at the pixel. Each pixel points to the neighbor with the lowest magnitude of the ratio of difference in intensity to difference in variance, and the pixels in the corresponding disjoint trees set their intensities to the mean of the root pixel (Figure 1).

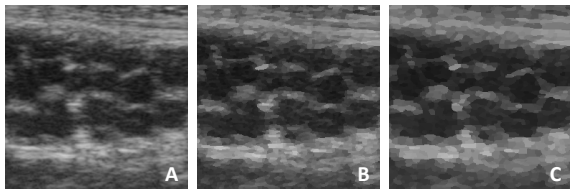


Figure 1. Construction of patches in 2D nerve image. (A,B,C) Original image of median nerve, image at radius 1 (pixel), and image at radius 3, respectively.

IDENTIFICATION OF BOUNDARY AND MEDIAL POINTS

Following construction of the new patches, we seek to describe the structures within the image while keeping the size of the data set within an order of magnitude of the patches. Each patch finds the point where a line drawn between its root and the root of a bordering patch intersects the boundary between them (Figure 2).

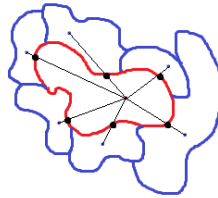


Figure 2. The red object is the patch in question, the blue objects are the neighboring patches, and the red and blue points are the roots of the objects, respectively. The boundary points identified by our approach are the black points, which represent the intersection between the line and the boundary.

Given this set of boundary points, we find medial points that lie equidistant from any two boundary points within a desired range of distances (Figure 3). For these medial points to form, the patches that the lines between the medial point and its two boundary points intersect must also meet a minimum threshold for homogeneity. Thus, medial points are a measure of association: the more medial points formed by the same pair of boundary points, the stronger the association between those boundary points.

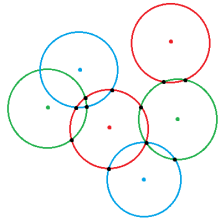


Figure 3. The red, blue, and green points represent individual boundary points while the red, blue, and green circles are shells of equal radius that have been formed around each of these boundary points, respectively. The black points in this diagram are the potential medial points, which are the intersections of these shells.

SEGMENTATION BY GROUPING

Utilizing this, boundary points are clustered into mutually exclusive boundary point sets through two steps. In the first step, the boundary points form a sparse graph, $G(N', E')$, by forming an edge from each boundary point (N') with its highest n associated boundary points, where n is user-defined. In the second step, the sparse graph is converted into a set of disjoint subgraphs by having each point form an edge to the point with the highest degree within a walk of length d , where d is user defined; all pre-existing edges are severed. The final step involves matching patches to boundary point sets by having each medial point within a patch vote for a boundary point set only if that set contains both of the boundary points associated with that medial point.

RESULTS

Figure 4. Segmentation of 2D ultrasound of nerve. (A,B) Original and segmented image of nerve. Fascicles are black structures with white borders. Compute time for a 256×256 image was < 1 second.

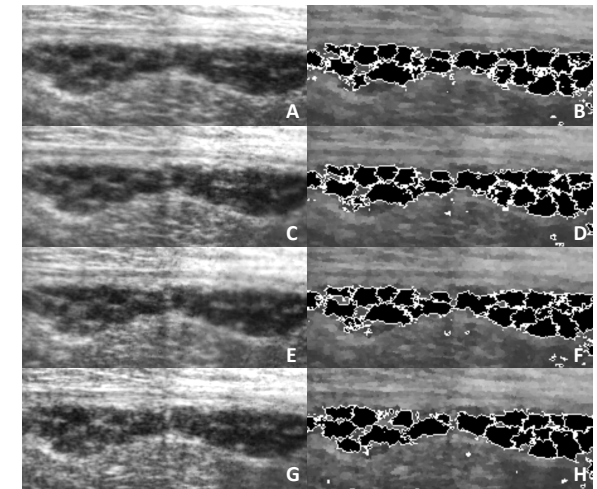
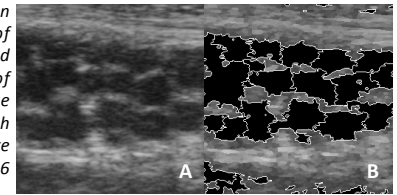


Figure 5. Segmentation of reconstructed 3D ultrasound of median nerve. (A,C,E) Three consecutive slices in original image of median nerve. (B,D,F) Corresponding segmentations of A,C, and E, respectively. Fascicle continuity is shown. (G) Slice of original image of median nerve at more distant location from slices in A,C, and E. (H) Corresponding segmentation of G. Fascicle continuity is still observed. In all images, fascicles are identified as black objects with white borders. Computation time for a $256 \times 256 \times 18$ image was < 7 seconds.

CONCLUSIONS

Our method has demonstrated effective segmentation of the median nerve in 2D and 3D in HRUS ultrasound data, with rapid computation times due to GPU implementation. Further optimization and development of these routines hold promise for our application of combining ultrasound analysis and video navigation in real time.